2000

Numerical Studies of Refrigerating Liquid Overfeed Systems Working with Ammonia and R-134a

O. Garcia-Valladares
Universitat Politecnica de Catalunya

C. D. Perez-Segarra
Universitat Politecnica de Catalunya

C. Oliet
Universitat Politecnica de Catalunya

S. Danov
Universitat Politecnica de Catalunya

NUMERICAL STUDIES OF REFRIGERATING LIQUID OVERFEED SYSTEMS WORKING WITH AMMONIA AND R-134a

O.García-Valladares, C.D.Pérez-Segarra, C.Oliet, S. Danov
Centre Tecnològic de Transferència de Calor (CTTC)
Laboratori de Termotècnia i Energètica; Universitat Politècnica de Catalunya
Colom 11, 08222 Terrassa (Barcelona), Spain
FAX: +34-93-739.81.01; Tel. +34-93-739.81.92
E-mail: labtie@labtie.mmt.upc.es

ABSTRACT

A numerical simulation of a liquid overfeed system working with pure refrigerants in steady state conditions has been performed. The global algorithm is based on the sequential resolution of the different elements of the system (compressor, evaporator, condenser, ...). For each element, a simplified mathematical model based on global balances of mass, momentum and energy is used. For the evaporator and condenser, specially tailored lumped parameter models have been developed based on an advanced detailed simulation model. In this way, global heat transfer coefficient (U) and the flow configuration factor (F) have been obtained. The behaviour of two refrigerant working fluids, ammonia and R134a, has been compared for a specified system and for different working conditions.

NOMENCLATURE

$\dot{W}$	power [W]
$\dot{Q}$	heat flux [W]
$\dot{m}$	mass flux [kg/s]
$\dot{m}_a$	oil mass flux [kg/s]
$\dot{m}_{aux}$	auxiliar heat exhanger secondary fluid mass flow [kg/s]
$\dot{m}_c$	condenser secondary fluid mass flow [kg/s]
$\dot{m}_e$	evaporator secondary fluid mass flow [kg/s]
α	heat transfer coefficient [W/m^2 K]
ρ	density [kg/m^3]
η	efficiency
λ	thermal conductivity [W/m K]
Δp	pressure drop [Pa]
ΔT_{lm}	logarithmic temperature difference [K]
ΔTsh	gas superheating [K]
Δz	height difference [m]
A	longitudinal area [m^2]
c_p	specific heat capacity cte press.[J/kg K]
D	diameter [m]
F	configuration factor
f	friction factor
g	acceleration due to gravity [m/s^2]
h	enthalpy [J/kg]
k	coefficient of pressure drop in singularities
m	mass [kg]
m_a	quantity of oil after the oil separator [ppm]
p	pressure [Pa]
S	cross section area [m^2]
T	temperature [K]
U	global heat transfer coefficient [W/m^2 K]
v	velocity [m/s]
X_a	oil mass fraction in low pressure receiver
x_g	vapour quality

subscripts

aux,i	inlet secondary fluid auxiliar heat exchanger
aux,o	outlet secondary fluid auxiliar heat exchanger
ins	insulation
c	condenser
c,i	inlet secondary fluid condenser
c,o	outlet secondary fluid condenser
cp	compressor
dis	discharge
E	electrical
e	evaporator
e,i	inlet secondary fluid evaporator
e,o	outlet secondary fluid evaporator
em	electrical-mechanical
ext	external
fric	friction
i	inner
numbers (1, 2, 3, ...) – points (see *Figure 1*)	
o	outer
p	pump
r	receiver
sing	singularities
suc	suction

INTRODUCTION

The objective of this paper is to study the thermal and fluid-dynamic behaviour of liquid overfeed systems. In these systems, two main circuits with different refrigerant mass flow rates are used. The circuits are joined by a liquid-vapour separator (also called the low pressure receiver) that supplies saturated liquid to the evaporator and saturated vapour to the compressor. In these systems, the liquid refrigerant is partially evaporated in the evaporator. A review of advantages and disadvantages of these systems is presented in (1).

A schematic representation of a overfeed system using a fin-and-tube evaporator is shown in *Figure* 1. Three main circuits can be seen. The first one from point 1 to 16 contains: compressor, oil separator, condenser, receiver, expansion device, tube connections and other elements (valves, bends, etc.). The second circuit, from points 101 to 107, contains: pump, fin-and-tube heat evaporator and tube connections. And the last one, from points 201 to 204 (optional oil return circuit), contains: a plate heat exchanger (oil distiller) and tube connections. The high-pressure side is from point 1 to 8; the rest of the points are in the low pressure side.

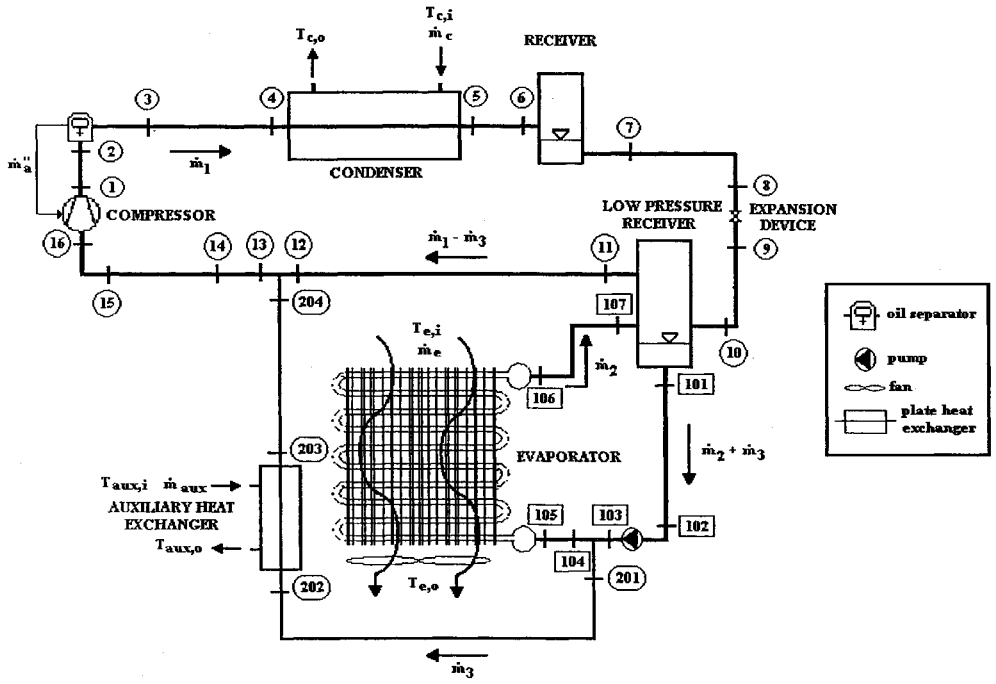

Figure 1. Liquid overfeed system circuit using a fin-and-tube evaporator.

A numerical simulation of a liquid overfeed system working with pure refrigerants in steady state conditions has been performed. The global algorithm is based on the sequential resolution of the different elements of the system (compressor, evaporator, condenser, ...). For each element, a simplified mathematical model based on global balances of mass, momentum and energy is used. The different elements of the system are modelized on the basis of global balances of mass, momentum and energy. The information needed to solve the compressor (power consumption, volumetric efficiency, heat losses, etc.) is empirically obtained. The same technique is applied to the pump. The condenser, evaporator and auxiliary heat exchanger are solved using the F-factor analytical method. Pressure drops and heat losses or gains in the connecting tubes are also taken into account. The simulation is capable to predict the operating point of the system in function of the equipment's characteristics and the prevailing thermodynamic conditions. Pressures, temperatures and mass and volumetric fluxes are calculated in all the points.

The global coefficients (global heat transfer coefficient, pressure drop coefficient, etc.) together with the influence of the flow configuration needed in the evaluation of some elements of the system (evaporator, condenser, ...) have been obtained from advanced numerical simulation models. Thus, higher level numerical

simulations have been employed in the heat exchangers (fin-and-tube and double-pipe heat exchangers) (2)(3). In these elements the governing equations of the flow (continuity, momentum and energy) are solved using a finite volume fully implicit step by step numerical scheme.

The thermal and fluid-dynamic behaviour of two refrigerant fluids, ammonia and R134a, has been studied for different boundary conditions. Global results such as the Molière diagram and some working parameters (evaporator capacity, compressor discharge temperature, pressure ratio, COP, mass flux through the compressor and the pump) are presented. The refrigerant's properties are evaluated using REFPROP v5.0 (4).

MATHEMATICAL MODEL

The present numerical model has been developed for steady state conditions and pure refrigerant fluids. The calculation of the refrigeration system is based on global energy, mass and momentum balances over the system's components. The three main circuits indicated in *Figure* 1 are: i) compressor circuit (point 1 to 16); ii) evaporator circuit (points 101 to 107); iii) auxiliary circuit for oil return (points 201 to 204). In this section, the equations used in these balances are presented for each element of the system.

Evaporator. A set of equations representing the global heat exchanged is obtained for the evaporator. The mass flux through the evaporator, the evaporator capacity and the outlet temperature of the secondary fluid are calculated from the following equations:

$$\dot{Q}_e = \dot{m}_2 (h_{106} - h_{105}) \tag{1a}$$

$$\dot{Q}_e = \dot{m}_e c_{p,e} (T_{e,i} - T_{e,o}) \tag{1b}$$

$$\dot{Q}_e = U_{oe} F_e A_{oe} \Delta T_{lm,e} \tag{1c}$$

$$h_{106} = f(p_e, x_{g106}) \tag{1d}$$

The outlet vapour mass fraction, x_{g106}, is obtained (assuming saturation conditions at the inlet section of the evaporator) from the circulating rate, x_{g106}=1/[circulating rate]. The global heat transfer coefficient and the flow configuration, $U_{oe}F_e$, is computed with the advanced numerical simulation developed for fin-and-tube heat exchangers (2). The inlet temperature $T_{e,i}$ and the mass flux $\dot{m}_e$ of the secondary fluid are known as boundary conditions. The circulation rate is fixed through the pump working frequency. The pressure drop through the evaporator is evaluated using the advanced numerical simulation, in this way a correlation function of the mass flux is developed for the evaluation of the pressure drop in different conditions.

Condenser. A set of equations representing the global heat exchanged is obtained for the condenser. The heat capacity in the condenser, the refrigerant outlet enthalpy and the outlet temperature of the secondary fluid are calculated from the following equations:

$$\dot{Q}_c = \dot{m}_1 (h_5 - h_4) \tag{2a}$$

$$\dot{Q}_c = \dot{m}_c c_{p,c} (T_{c,i} - T_{c,o}) \tag{2b}$$

$$\dot{Q}_c = U_{oc} F_c A_{oc} \Delta T_{lm,c} \tag{2c}$$

$$h_5 = f(p_5, T_5) \tag{2d}$$

The global heat transfer coefficient and the flow configuration, $U_{oc}F_c$, is computed with an advanced numerical simulation. The inlet temperature $T_{c,i}$ and the mass flux $\dot{m}_c$ of the secondary fluid are known as boundary conditions. The pressure drop in the condenser is evaluated in the same way that was explained in the evaporator.

Compressor. The mechanical power applied to the fluid in the compressor ($\dot{W}_{cp}$) and the discharge temperature and enthalpy (T_1, h_1) are obtained from an energy balance and the relationship between the electrical power and the mechanical power applied to the refrigerant,

$$\dot{W}_{cp} = \dot{W}_E \eta_{em} \tag{3a}$$

$$\dot{W}_{cp} = \dot{m}_1 (h_1 - h_{16}) \tag{3b}$$

$$h_1 = f(p_1, T_1) \tag{3c}$$

The compressor is characterized by:

Electrical power consumption: $\dot{W}_E = f($ compressor type, fluid, p_{dis}, $p_{suc})$ (3d)

Electrical-mechanical efficiency: $\eta_{em} = f($ compressor type, fluid, $p_{dis}/p_{suc})$ (3e)

Mass flux: $\dot{m}_{cp} = f($ compressor type, fluid, p_{dis}, p_{suc}, $\Delta Tsh_{suc})$ (3f)

For the selected compressor and refrigerant fluid, two matrices are generated using the manufacturer's data, one of values for the mass flux and another for the electrical power consumption in function of the suction and discharge pressure. When a value between the calculated matrix points is required, it can be obtained by interpolation between the nearest 4 points.

Expansion device. The expansion mechanism is considered adiabatic (h_9=h_8).

Pump. The power applied from the pump to the fluid ($\dot{W}_p$) is obtained data from the manufacturer's pump characteristic curves. In this way the outlet enthalpy (h_{103}) in the pump is obtained from an energy balance,

$$\dot{W}_p = (\dot{m}_2 + \dot{m}_3)(h_{103} - h_{102}) \tag{4}$$

Receiver. If the receiver is considered adiabatic, the outlet condition in this element corresponds to saturated liquid at its corresponding pressure due to the system working conditions.

Low-pressure receiver. In this element, with two inlets and two outlets, the conditions of points h_{101} and h_{11} are saturated liquid and saturated vapour at the pressure of the low-pressure receiver. With this information and from an energy balance, the point h_{101} or the point h_{11} is obtained, and from this, the pressure in the low-pressure receiver is calculated.

$$\dot{m}_1 h_{10} + \dot{m}_2 h_{107} + \dot{Q}_r = (\dot{m}_2 + \dot{m}_3) h_{101} + (\dot{m}_1 - \dot{m}_3) h_{11} \tag{5a}$$

$$h_{101} = h_{l,sat}(P_{101}) \tag{5b}$$

Tubes and singularities. For each section between two points in the *Figure 1*, that only includes tubes and singularities, the heat loss or gain and the pressure drop are calculated from the following equations:

$$U_i A_i \Delta T_{lm} = \dot{m}\left(h_{out} - h_{in}\right) \tag{6a}$$

$$\left(p_{out} - p_{in}\right)S - \Delta p_{fric} A - \Delta p_{sing} A - mg\Delta z = \dot{m}\left(v_{out} - v_{in}\right) \tag{6b}$$

The pressure drop in each section is due to flow friction Δp_{fric} and local pressure drop through singularities (valves, contractions, expansions, bends, etc.) Δp_{fsing}:

$$\Delta p_{fric} = f\frac{\rho v^2}{2} \tag{6c}$$

$$\Delta p_{sing} = k\frac{\rho v^2}{2} \tag{6d}$$

For the calculation of the friction factor (f) inside the tubes and pressure drop factor (k) through singularities, different empirical correlation considering single or two-phase flow have been used. For the calculation of the heat

fluxes in the tubes, the global heat transfer coefficient in each one is calculated considering the inner and outer heat transfer coefficients (α_i and α_o) and the thermal resistances of the tube and the insulation.

$$U_i = \left[\frac{1}{\alpha_i} + \frac{D_i}{2\lambda_{ins}} \ln\left(\frac{D_{ext}}{D_o}\right) + \frac{D_i}{2\lambda_{tube}} \ln\left(\frac{D_o}{D_i}\right) + \frac{D_i}{D_o \alpha_o} \right]^{-1} \quad (6e)$$

For the computing of the inner heat transfer coefficient α_i, correlations for single and two-phase flow have been used. For the outer coefficient α_o, natural convection around tubes has been considered.

Calculation of additional mass fluxes. In the case of halocarbons, the mass flux $\dot{m}_3$ is calculated supposing that the whole quantity of oil after the oil separator is returned to the compressor from the auxiliary circuit, preventing in this way malfunctioning of the compressor. The quantity of oil passing through the oil separator (m_a) (in parts per million (ppm)), and the quantity of oil in the low pressure receiver (X_a) (mass of oil/[mass of oil + mass of refrigerant]) are data given by the oil separator characteristics and for the established working conditions in the unit.

$$\dot{m}_a = \frac{m_a \dot{m}_1}{1 \times 10^6} \quad (7a)$$

$$\dot{m}_3 = \dot{m}_a / X_a \quad (7b)$$

Auxiliary heat exchanger. A set of equations representing the global heat exchanged is obtained for the auxiliary heat exchanger. The heat capacity in this element, the mass flux and the outlet temperature of the secondary fluid are calculated from the following equations:

$$\dot{Q}_{aux} = \dot{m}_3 (h_{203} - h_{202}) \quad (8a)$$

$$\dot{Q}_{aux} = \dot{m}_{aux} c_{p,aux} (T_{aux,i} - T_{aux,o}) \quad (8b)$$

$$\dot{Q}_{aux} = U_{oaux} F_{aux} A_{oaux} \Delta T_{lm,aux} \quad (8c)$$

At the outlet of this heat exchanger, the superheating (h_{203}) needed to evaporate the refrigerant and to drag the oil to the compressor is fixed. The global heat transfer coefficient and the flow configuration, $U_{oaux}F_{aux}$, is specified (usually from an advanced numerical simulation). The inlet temperature $T_{aux,i}$ of the secondary fluid is known as boundary conditions. The pressure drop in the auxiliary heat exchanger is evaluated in the same way as was explained in the evaporator.

Moreover, in the node where points 12 and 204 connect with point 13, another energy balance is made to evaluate h_{13}.

Global algorithm. Beginning with an initial value of the suction and discharge pressure of the compressor, all the enthalpies and pressures are computed for each element iterating until convergence is reached. Variables like velocities are also calculated to ensure that the design of tubes dimension are correct. *Figure 2* shows the flow diagram for the resolution of the complete liquid overfeed system.

NUMERICAL RESULTS

The performance of different modes of operation and different working fluids can be compared on the basis of either internal parameters (i.e. condensing and evaporating temperatures), or external parameters, such as the inlet temperature of the heat transfer secondary fluids. The latter approach is chosen for this work because this situation is more likely in real life (when the heat source and the heat sink temperatures are fixed) (5).

The numerical simulation test for R134a and ammonia are performed at one heat sink temperature 33°C ($T_{c,i}$), because an oversize condenser has been selected with the objective of controlling this parameter in the

experimental unit. For this fixed condenser temperature, the heat source temperature ($T_{e,i}$) in the evaporator is set at different values (from –7.5 to 10°C). A circulation rate of 4 is fixed in the evaporator. Test on the R134a is run at the same conditions as for ammonia. For R134a, the quantity of oil passing through the oil separator (m_a) is assumed 50 ppm and the oil mass fraction in the low pressure receiver (X_a) is also assumed as $1x10^{-3}$.

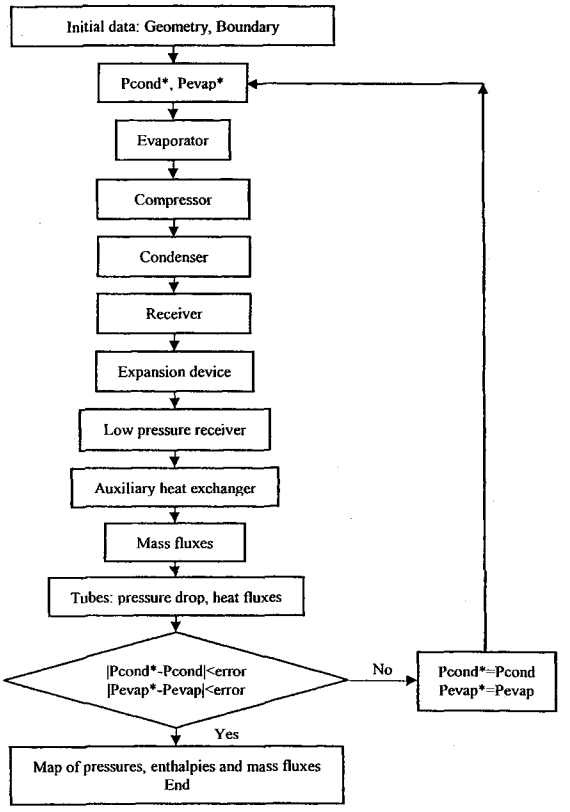

Figure 2. Flow diagram for the resolution of the liquid overfeed system.

The parameters chosen to describe the system's performance are: pressure ratio across the compressor (p_{dis}/p_{suc}), compressor discharge temperature, evaporator rating capacity ($\dot{Q}_e$), COP ($\dot{Q}_e/\dot{W}_{cp}$) and mass fluxes through the compressor and pump. Moreover, thermodynamic characteristics of the liquid overfeed systems working with the same fluid and different working conditions are here presented on the basis of the pressure-enthalpy diagram (Molierè diagram).

The performance of the R134a and ammonia in the liquid overfeed system is compared. As expected due to the better thermodynamic properties of ammonia, the evaporator's refrigerating capacity is higher for ammonia and needs less mass flux than in the case of R134a (ammonia has a high latent heat of vaporisation, so for equal heat removal, much less ammonia mass must be circulated compared to halocarbons) as shown in *Figure 3*. Although the COP is smaller because the compressor power supply is higher for ammonia than for R134a, according to the manufacturer's data; Therefore, the discharge temperature is also much higher than for R134a. Moreover, the pressure ratio is also higher for ammonia.

A thermodynamic comparison between the R134a and ammonia performed for different heat source temperatures is illustrated in the Molière diagrams in *Figure 4*. In these diagrams, the much higher latent heat of vaporisation for the ammonia is observed (difference between the enthalpies in the liquid and vapour saturation curves) and its higher pressure working conditions. The symbols in the figures represent the points of pressures and enthalpies calculated by the numerical simulation. For all these points, flow variables are calculated (velocities, mass fluxes, enthalpies, temperatures, pressures, mass fractions, void fractions).

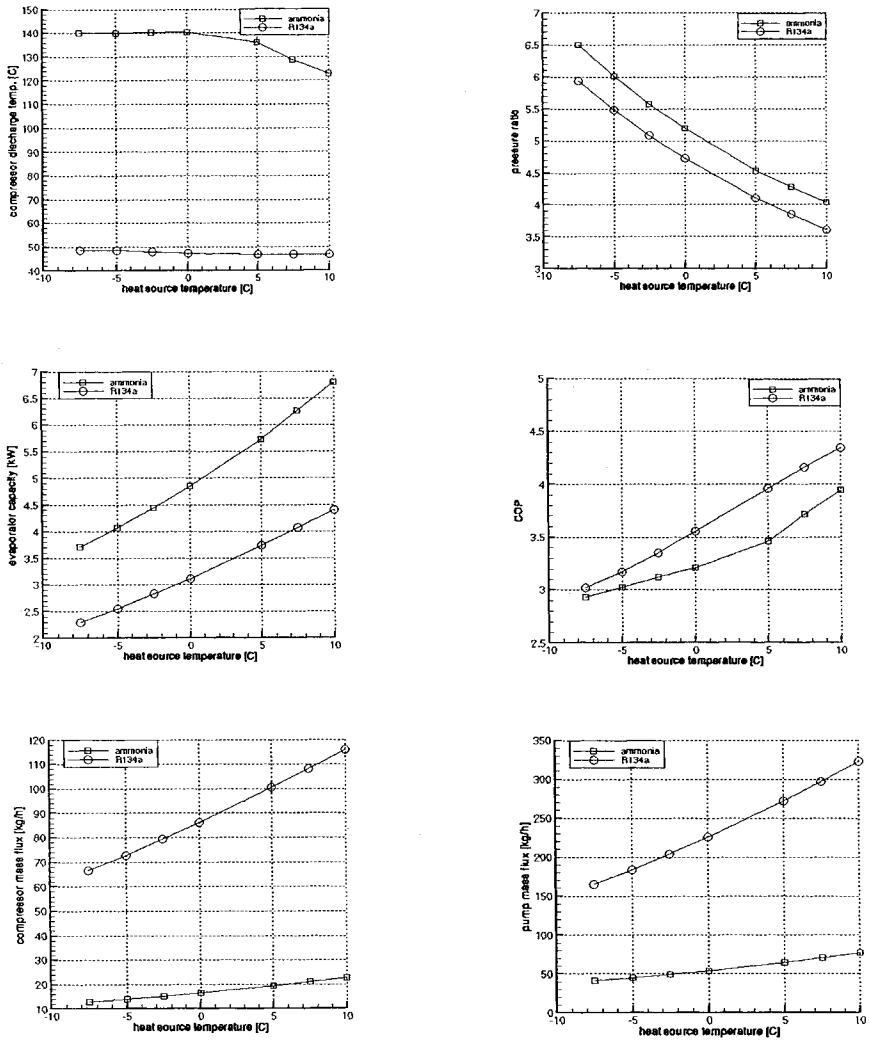

Figure 3. Comparison between the performance of R134a and ammonia in a liquid overfeed system.

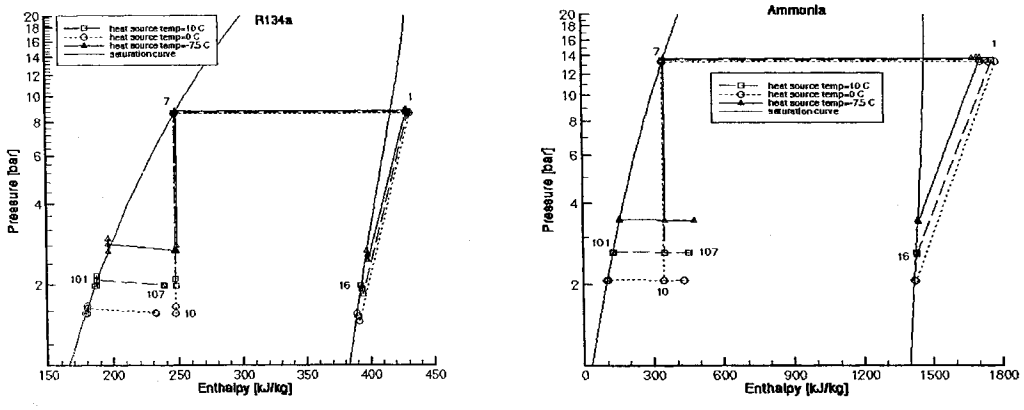

Figure 4. Comparison between the thermodynamic cycles performed by R134a and ammonia for 3 different heat source temperatures in a liquid overfeed system.

CONCLUSIONS

A numerical simulation of a liquid overfeed system working with pure refrigerants in steady state conditions has been performed. The global algorithm is based on the sequential resolution of the different elements of the system (compressor, evaporator, condenser, ...). For each element, a simplified mathematical model based on global balances of mass, momentum and energy is used. For the compressor, the pump and other elements, the characteristic curves of the component are used. For the evaporator and condenser, specially tailored lumped parameter models have been developed based on an advanced detailed simulation model. In this way, global heat transfer coefficient (U) and the flow configuration factor (F) have been obtained. The behaviour of two refrigerant working fluids, ammonia and R134a, has been compared for a specified system and for different working conditions. The influence of the heat source and heat sink temperatures in both systems behaviour has been shown.

ACKNOWLEDGEMENTS

The authors would like to express their thanks to Mr. Daniel Hernández, from TEFRINCA, for their technical support. This work has been financially supported by the Spanish Government (project TIC99-0770) and by the European Community (project JOE-CT98-7021 (DG12-GIGO)).

REFERENCES

(1) 1994 ASHRAE HANDBOOK, REFRIGERATION Systems and Applications, SI Edition, Chapter 1 Liquid Overfeed Systems, ASHRAE Inc.

(2) Oliet, C., Pérez-Segarra, C. D., García-Valladares, O., Ordoñez, R., Sudrià, J. (1998), Diseño Termo-fluídico de Intercambiadores Compactos gas-líquido. Aplicación a Radiadores de Automoción y Evaporadores. XIII Congreso Nacional de Ingeniería Mecánica, Vol 4, pp.581-587. Barcelona, Spain.

(3) García-Valladares, O., Pérez-Segarra, C.D., Rigola, J. y Oliva, A. (1998), Detailed Numerical Simulation of Condensers and Evaporators using Pure and Mixed Refrigerants, Int. Compressor Eng. Conference at Purdue Univ., 2, pp.839-844.

(4) REFPROP v.5.0 (Feb 1996), NIST Thermodynamic Properties of Refrigerants and Refrigerant Mixtures Database, Standard Reference Data Program, Gaithersbug, MD 20899, USA.

(5) Giuliani, G., Hewitt, N. J., Marchesi Donati and Polonara, F. (1999), Composition in liquid-recirculation refrigerating systems: an experimental investigation for the pure fluid R134a and mixture R32/R134a, International Journal of Refrigeration, Vol. 22, pp.486-498.